

Evolution and Intersection of Extended Defects and Stacking Faults in 3C-SiC Layers on Si (001) Substrates by Molecular Dynamics Simulations: The Forest Dislocation Case

*Luca Barbisan, Emilio Scalise and Anna Marzegalli**

L. Barbisan, Dr. E. Scalise

L-NESS

Department of Materials Science

Università degli Studi di Milano-Bicocca

via R. Cozzi 55, I-20125 Milano, Italy

Dr. A. Marzegalli

L-NESS

Department of Physics

Politecnico di Milano

via Anzani 42, I-22100 Como, Italy

E-mail: anna.marzegalli@unimib.it

Keywords: extended defects, forest dislocations, electronic properties, molecular dynamics, cubic silicon carbide, stacking faults, ab-initio calculations

The crossing of stacking faults (namely dislocation forests) in 3C-SiC have been experimentally probed to cause detrimental effect on the electronic properties of the layer. By means of classical molecular dynamics simulations, we show for the first time the evolution of two crossing partial dislocation loops, revealing the mechanism that leads to the formation of a complex defect at their intersection. The obtained atomistic structure is then further refined by ab-initio calculations, revealing that this defect does not cause defect states within the gap of the pristine material.

We investigate also the case of the intersection of two double dislocations loops, i.e. involving double stacking faults, in the hypothesis that the evolution follows the same mechanism found for single dislocation loops. Contrary to the single plane intersection, our simulations reveal that the junction formed by double dislocation loops does cause intra-gap states, thus suggesting detrimental effects on the electronic properties of the 3C-SiC layers.

1. Introduction

Cubic silicon carbide (3C-SiC) is one of the most suitable materials for innovation in high power and high-frequency electronic device industries,^[1-5] due to its unique physical and chemical properties. In particular, 3C-SiC combines a large bandgap value (2.35 eV),^[6] high bulk and channel electron mobility (up to 1000 and 250 cm² /Vs, respectively),^[7,8] and low trap density at the 3C-SiC/SiO₂ interfaces of the metal-oxide-semiconductor structures.^[9] Nowadays, a technique able to obtain a large area bulk 3C-SiC material is still lacking and the epitaxial deposition of cubic silicon carbide on Si substrate is mostly used. On one hand, this allows the direct integration of 3C-SiC in the Si technology,^[10] on the other hand, SiC epilayers suffer from quality issues due to the structural differences between the two materials. Indeed, their lattice parameters differ by about 20% at room temperature and their thermal expansion coefficients of about 8%.^[8] Consequently, several types of defects, such as dislocations, twins, antiphase boundaries (APBs), and stacking faults (SFs), nucleate in the SiC epilayer to relax the misfit and thermal strain both during the deposition than the cooling down.^[11,12] A high density of these defects hinders the possible practical use of 3C-SiC epilayers having detrimental effects on the performance of devices, particularly on the leakage current and breakdown electric field.^[13-20] Attempts for defect reduction, such as growth on misoriented and patterned substrates,^[16,19-23] lead to the conclusion that SFs, differently from the other kind of defects, cannot be completely eliminated due to their continuous generation during the growth^[24-26] and that their presence, even in the low densities achieved (of the order of 10⁴ cm⁻¹)^[27,28] has a detrimental impact on the electrical layer properties.^[13-20,29-32] However, it is an open question whether the SFs per se are responsible for the detrimental leakage currents because they are theoretically predicted to introduce no mid-gap electronic states in the 3C-SiC phase.^[33,34] SFs are unavoidably associated with partial dislocations, bounding them. In Ref. [35] it has been demonstrated via an ab-initio calculation that partial dislocation complexes terminating multiple SFs cause the appearance of defect states filling the bandgap of 3C-SiC. Moreover, partial dislocations drive the nucleation and enlargement of the faulted planes, inducing their shape,^[20,36] and several defect configurations were observed experimentally to be caused by the dislocation interaction.^[37,38] It has been proposed that a high density of crossing SFs (called dislocation forests) can have a detrimental impact on the electronic properties of 3C-SiC epilayer,^[27] so that they could be considered as killer defects in 3C-SiC together with the dislocation complexes.^[35]

In this paper, a multiscale approach combining classical molecular dynamics (MD) simulations and ab initio calculations, has been used to study the crossing of stacking faults in 3C-SiC epitaxial layers. The two methods resulted to be complementary in the description of the formation of defective complexes and the identification of the corresponding impact on the quality of the material in terms of electronic performances. We show that the imaging of two crossing SFs has to be interpreted as the result of the intersection of two adjacent partial dislocation loops that are opening along the same $\langle 110 \rangle$ direction in two different $\{111\}$ planes. Indeed, under tensile strain, they can intersect and continue their motion giving rise to a new line defect at their crossing point. Actually, the two SFs intersect and continue to expand while the partial dislocations bounding them remains first pinned at the crossing point, change their line directions, and give rise to the formation of the new defect after depinning. The defect structure corresponds to the deposition of four 90° dislocation segments above and below the two SFs. Ab initio calculations demonstrate that defect states in the middle of the band gap appear if the crossing SFs consists of multiple planes as in the case of the dislocation complexes terminating multiple dislocation loops.

2. Computational Methods

We performed classical molecular dynamics simulations using the software Large-scale Atomic/Molecular Massively Parallel Simulator (LAMMPS) [39] and Vashishta interatomic potential.^[40] Vashishta potential has some advantages over other empirical potentials for silicon carbide:^[41] this potential considers the atom interactions beyond the first neighbour shells, therefore different total energies for the hexagonal and the cubic configurations are provided, thus enabling for an estimate of nonzero stacking fault energies. The simulations are performed in the canonical (i.e., the number of particles, the volume and the temperature are constant, NVT) ensemble, using a Nose–Hoover thermostat.^[42] The atomic trajectories were analysed using the Open Visualization Tool (OVITO) software,^[43] which identifies extended defects in virtual crystals, highlighting SFs and dislocation lines along with the associated Burgers vectors. Orthogonal simulation cells, oriented along the directions determined by the vectors $u = a/2 [1\bar{1}0]$, $v = a/2 [110]$, and $w = a [100]$ were used, and periodic boundary conditions (PBCs) were applied in the u and v directions. The bottom three layers in the simulation cell were fixed at the atomic position of the bulk, to model the effect of the Si substrate below the 3C-SiC layer. A large box ($38.8 \times 38.8 \times 26.0 \text{ nm}^3$ corresponding to $3'456'000$ atoms) was needed to analyse the evolution and interaction of multiple dislocations.

Dislocation loops were inserted in the simulation cell by shifting each atom according to the displacement field vectors calculated by the dislocation theory in the framework of the linear elasticity theory.^[44] The obtained configurations were geometrically optimized using a conjugated gradient minimization algorithm. For an arbitrary dislocation segment, the field components can be calculated by rotating the reference system and decomposing the dislocation Burgers vector into a screw (b_{\parallel}) and an edge component (b_{\perp}). At this, \hat{z} axis has to be oriented along the dislocation line ξ , \hat{x} axis perpendicular to ξ in the glide plane, and \hat{y} axis oriented following the right-hand rule, respectively. In this case, the components of the displacement field vectors turn to be the following

$$u_x(x, y, z) = \frac{b_{\perp}}{2\pi} \left(\arctan(y, x) + \frac{xy}{2(1-\nu)(x^2+y^2)} \right) \quad (1)$$

$$u_y(x, y, z) = -\frac{b_{\perp}}{2\pi} \left(\frac{(1-2\nu)\log(x^2+y^2)}{4(1-\nu)} + \frac{x^2-y^2}{4(1-\nu)(x^2+y^2)} \right) \quad (2)$$

$$u_z(x, y, z) = \frac{b_{\parallel}}{2\pi} \arctan(y, x) \quad (3)$$

where ν is the Poisson ratio of 3C-SiC.^[45] Notice that the displacement field components (1)–(3) have to be corrected to have the stress normal to the free surface equal to zero after system equilibration. This has been done by adding an image dislocation loop in the vacuum above the free surface.^[44] The annealing of the systems was carried out at the thermostat temperature of 1400 K, corresponding to the typical experimental temperature for 3C-SiC deposition. The integration time step was one fs. Moreover, we scaled the simulation box dimensions by a factor calculated using the Nose–Hoover barostat, to avoid the presence of residual strain due to the thermal dilation of the layer.

The electronic structure calculations are based on density functional theory (DFT) and exploit the recently developed non-empirical strongly constrained and appropriately normed (SCAN) meta-GGA functionals. Further details on the DFT calculations can be found in our previous work,^[35] where the partial dislocation complexes terminating multiple SFs and their electronic defect states were investigated.

3. Results and Discussion

Looking at the interaction between SFs, several structural configurations can be probed.^[27,37,38] In particular, it has been suggested that forest dislocations lead to deleterious effects in the electronic properties of the layer,^[27] but a study of the atomistic structure of these defects and of its relative electronic properties is still lacking.

In this section, we present novel results on dislocation forest divided in two sections: in the first one, we show molecular dynamic simulations of the evolution of crossing loops leading to the formation of a dislocation forest, into the second atomistic details of the complex defect thus formed are presented, and their relative electronic states obtained by ab initio calculations are discussed.

3.1. Evolution of crossing SFs and formation of dislocation forest

Forest dislocations are complex defects that form at the intersection of two expanding dislocation loops whose threading arms cross each other. Due to the mismatch with the substrate, the cubic SiC layer is in a tensile state in the first deposition stages. In this case, 90° partial dislocations parallel to the interface are known to take part in the strain relaxation,^[31] creating SFs within the layer.

Following the procedure described in the previous section, we construct in our cell two dislocation loops with Burgers vector $\vec{b} = \frac{a}{6} [112]$ and $\vec{b} = \frac{a}{6} [11\bar{2}]$ lying on (111) and $(11\bar{1})$ planes, respectively. Loops are placed consecutively, one close to the other with the segment parallel to the interface along the same $[\bar{1}10]$ direction. Being the loop constituted by partial dislocation segments in its internal part, a stacking fault is present. Such initial configuration is shown in panel (a) of **Figure 1**. Loops have initially a hexagonal shape due to the fact that the preferred dislocation lines in the zincblende structure are $\langle 110 \rangle$ in type, so that six favoured dislocation segments are present on each $\{111\}$ planes. Consequently, dislocation segments that are not parallel to the interface turn to be 30° partial dislocations. Immediately the evolution computed by MD changes the loop shape making them more rounded (see also Ref. [36]). We applied a tensile strain of 4% in the cell. The value of such strain is set to be sufficient to observe the loops evolve in a reasonable computational time but not too high to lead to disorder in the cell (as in Ref. [36]). Indeed, the main part of the relaxation of the initial 20% misfit strain in the layer is known to be done by an array of Lomer dislocations formed in the first deposited layers as a structural reconstruction directly at the interface.^[31] So, it is impossible to correctly estimate the real strain acting in the loop opening being dependent on the local formation of Lomer dislocations. The two loops expand as shown in the panel (b) driving two threading arms one close to the other. When they reach, a junction is developed as shown in Figure 1d by an enlarged image of the crossing configuration. Upon further evolution we can observe that the dislocations do not cross the stacking fault plane of the encountered loop. Instead, each threading dislocation remains pinned at the junction point, changes locally the dislocation line direction, and deposits two

segments parallel to the interface, as shown in Figure 1e, where the threading arms are coloured differently (light blue and red) to clarify the mechanism. Then threading dislocations further move apart via a depinning process and leave a complex line defect along the junction. The visualization program OVITO cannot resolve it, therefore a white cylinder is drawn in the simulation. However, the resolved defect structure can be easily analysed by cutting a slice along the intersection line (white cylinder) and looking along those lines reported in **Figure 2a**. Clearly, forming the junction, the threading arms change their direction, also changing the angle between the Burgers vector and the dislocation lines, i.e. the dislocation type. Each segments becomes a 90° dislocation as all the segments parallel to the interface. As a consequence, the new complex defect developed, namely the forest dislocations, turn to be formed by four adjacent 90° dislocations and two SFs, as seen in Figure 2b. The four composing 90° dislocation cores are highlighted in red in panels (c-f) of Figure 2.

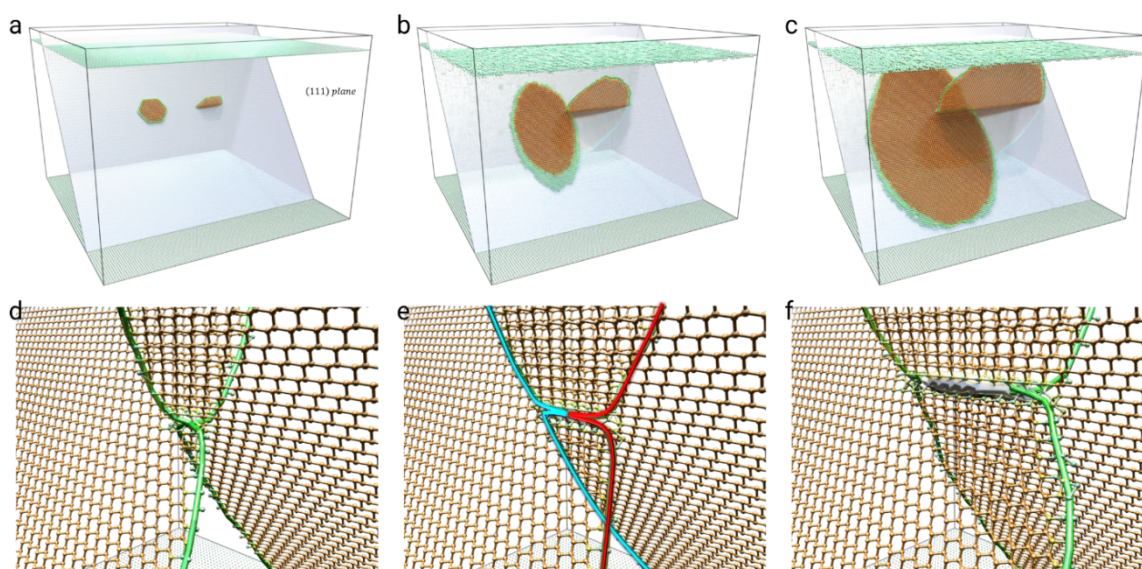


Figure 1: Dislocation Forest formation mechanism. Orange atoms belong to the SFs and in green are drawn the dislocation lines. Panel a): initial configuration for MD simulations (one $\{111\}$ habit plane of one loop is highlighted together with the surface and interface); panels b) and c) snapshots of the loop evolution computed by MD showing their intersection; panel d) enlargement view of the pinning point at the simulation time of the initial crossing; panel e) enlargement view of the junction formation in its initial stages (the two different threading dislocations are coloured in light blue and red); panel f) junction configuration developed after threading dislocation depinning.

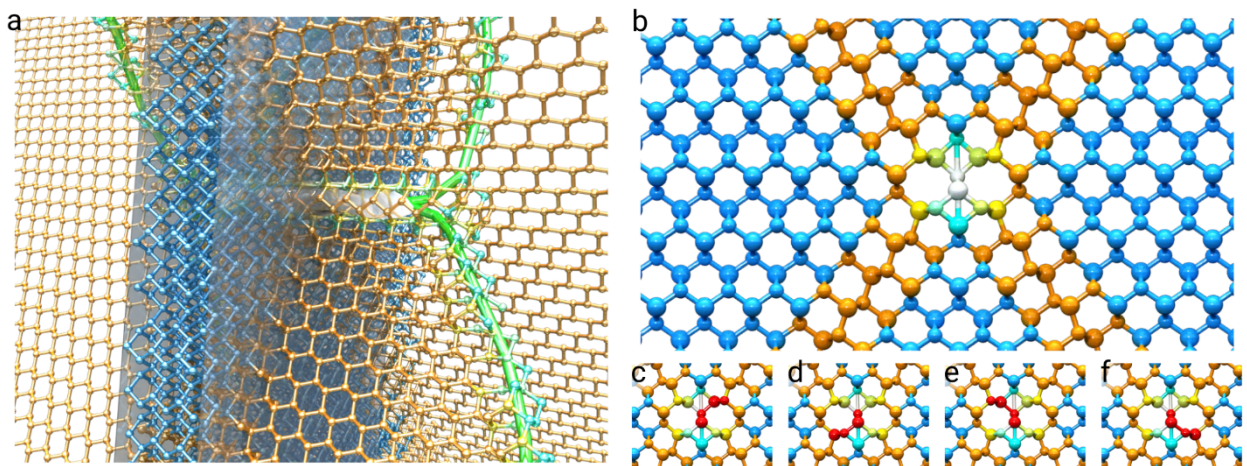


Figure 2: Analysis of the junction structure: Panel a) view of the cut plane considered (light blue atoms are in the perfect cubic lattice, orange atoms belong to SFs, in green are the dislocation lines); panel b) the projected view in $\langle 110 \rangle$ direction of the junction structure (white and coloured atoms, except to orange and light blue, do not belong to any recognized crystal structure); panels (c-f) are zoomed images of the junction core and atoms highlighted in red can be associated to the four 90° dislocation segments cores.

In Ref. [27], it is clearly shown that the highest abundance of SFs near the interface of 3C-SiC layers on Si(001) substrates turns to be multiple-plane SFs. In Ref. [35] it is proposed a mechanism for the formation of double and triple SFs via gliding of adjacent Shockley partials. It is validated by MD simulations of the evolution of only the segments parallel to the interface. It is almost impossible to follow the evolution of entire multiple loops in three dimensions in reasonable computational time. But it can be supposed that also multiple SFs can intersect each other, as illustrated above (Figure 1) for the single loop. In particular, double SFs are composed of adjacent 30° and 90° partial loops, forming a defect with 30° total Burgers vector, and therefore it can further evolve. In contrast, triple SFs have a null total Burgers vector so that they do not move and their intersection is statistically less probable.^[35]

In analogy with the mechanism found by simulation for single loops, we construct in a periodic cell also the complex defect that should appear at the intersection of double SFs. It is shown in **Figure 3** panel (a). Notice that the cell is tilted in order to recover the full periodicity. Eight partial dislocation segments parallel to the interface are inserted in the cell,

30° and 90° in type. The procedure has been illustrated by showing the four different double partial dislocations inserted in the four panels on the right. Red atoms belong to 90° partial dislocation cores, while green and pink atoms to 30° partial dislocation and are antiparallel in the screw component. Each double dislocation shown in each panel corresponds to one of the two segments deposited in the junction by one of the crossing threading arms of the double loop after depinning. Panels (b) and (c) show the segments relative to the threading traveling in a $\{111\}$ plane and (d) and (e) to the threading traveling in the other. The cell has been then relaxed by a conjugated gradient procedure using Vashista potential.

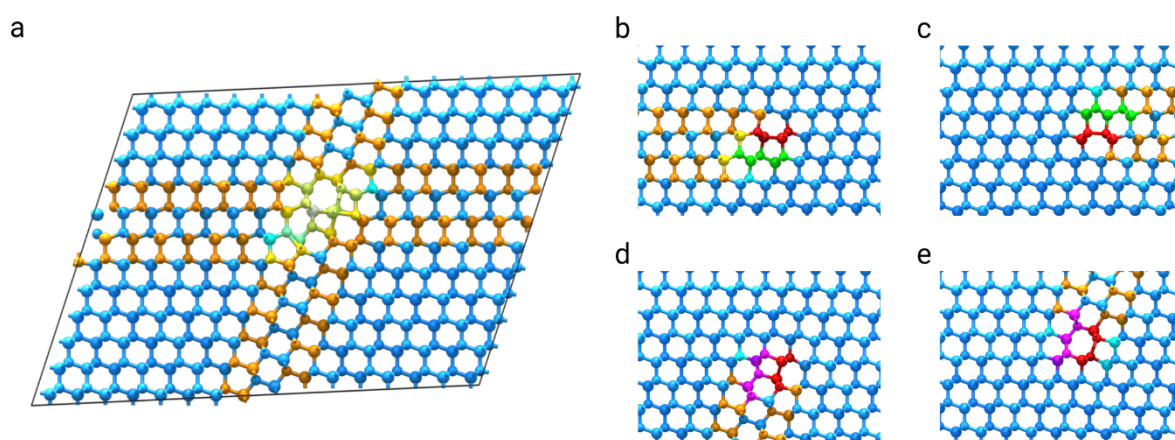


Figure 3: Structure of the junction developed by two crossing double SFs. Panel a) view of the structure constructed in a periodic cell; panel b) and c) double dislocation segments inserted in the cell in a) as due to the depinning of one of the threading of the double loop (like light blue in Figure 1e); panel d) and e) double dislocation segments inserted in the cell in a) as due to the depinning of the other threading (like red in Figure 1e)

Established the realistic atomistic structures of forest dislocations, we used them in a superior ab-initio calculation to further relax the structure and analyse their electronic properties.

3.2. Electronic properties of dislocation forests

The electronic density of states (DOS) calculated for an intersection between the single loop is shown in **Figure 4**. The simulation cell has been built periodic, inserting the structure of the junction obtained by classical MD simulations developed by two crossing double SFs shown in Figure 3, in order to facilitate the DFT calculations. A ionic relaxation has been performed by DFT. Then, the DOS has been calculated and integrated inside 20 slices of the cell and plotted as a function of the energy (with respect to the calculated Fermi energy) and its

intensity, whose color scale is also shown in Figure 4. The integrated DOS in each slice is plotted along one of the directions of the cell, and specifically the horizontal one is shown in the corresponding atomistic model of Figure 4. This approach may help to identify possible defective electronic states in the bandgap of the material and localize them within a real space region in the crystal cell model. The calculated DOS shows quite clearly that the single SF does not introduce any relevant electronic state in the bandgap of the 3C-SiC. In fact, far from the central region plotted in Figure 4, the bandgap is very close to our predicted gap for bulk 3C-SiC (of about 1.9 eV), in agreement with our previous findings.^[35] In the central region of the cell modeled, corresponding to the intersection zone between the two SFs, a few states appear, close to the valence band edge. However, these states may be identified as very shallow states, similarly to the states found for the dislocation complex terminating the single SFs,^[35] thus they should not be very detrimental for the devices.

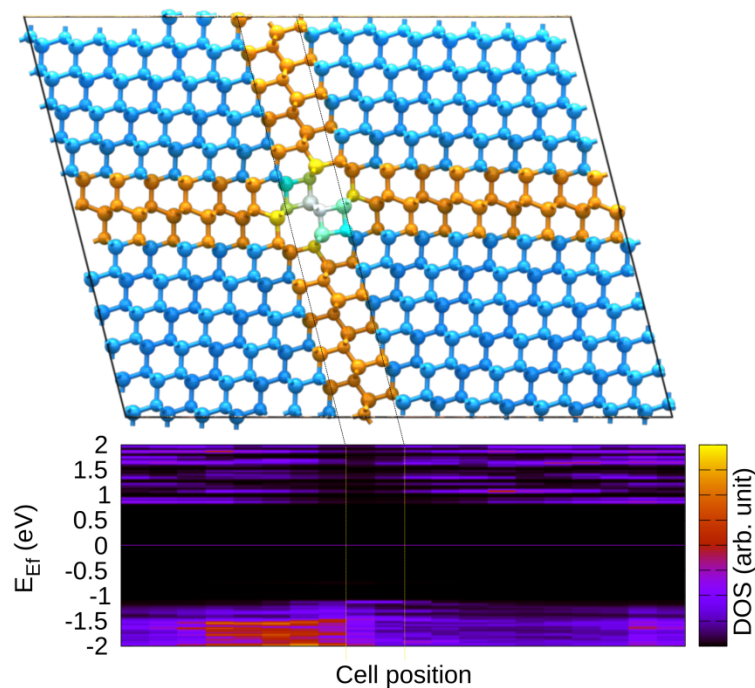


Figure 4: Electronic density of states (integrated in boxes) for the intersection between single loops, whose atomistic model is illustrated in the top graph. A central slice of the simulated cell, centred at the crossing point, is marked by dotted lines, and also highlight the corresponding position in the DOS plot. The colours of the atomistic structure agree with the previous images.

The same approach has been used to investigate the electronic properties of the intersection between two double SFs. Contrary to the single loops case, the DOS of the intersection

between double SFs, illustrated in **Figure 5**, shows several defect states with the bandgap of the pristine material. These intra-gap states are in energy just a few hundreds of meV one from each other and spatially very localized at the intersection point. Thus, their impact on the electronic transport and particularly on the leakage current into the device may be marked, as also already shown for the dislocation complexes terminating the double SFs.^[35] A deeper analysis on the physical origin of these intra-gap states needs for a further and specific study which is out of the scope of this paper, but few important points may be highlighted here. The two states above the Fermi level and well below the conduction band edge are induced by the dangling bonds of the C atoms close to the intersection point. In our previous work^[35] we have found that typically C-C bonds involved in the reconstruction of the dislocation core are not responsible for deep intra-gap states, but we see here that the C dangling bonds act differently. In fact, by pushing closer the two C atoms, each with a dangling bond in the atomic structure of Figure 5, a new reconstruction is formed after ionic relaxation. A comparison between the two structures, revealed that the induced C-C bond is very stretched and thus less stable (proved by an higher total energy of the simulated cell) than the structure shown in Figure 5 and including the dangling bonds. However, the two intra-gap states above the Fermi level disappear when the C-C bond is formed, but the other intra-gap states below the Fermi level remains unaffected. Note that the discrete states that we are commenting here are very likely single dispersive states if plotted along the k-space, as already shown for the dislocation complexes.^[35] Note also that our analysis does not include charged defects, thus further analysis is necessary to study exhaustively the stability of these structures and understand how this may impact on the defect states. Nevertheless, the appearance of the intra-gap states below the Fermi level in both the different reconstructions simulated, suggests that they are unaffected by the specific reconstructions that may be formed at the intersection of the two double SFs. Therefore, they are very likely to cause detrimental effects on the performance of the SiC devices, in analogy with the dislocation complexes terminating double and triple SFs.^[35]

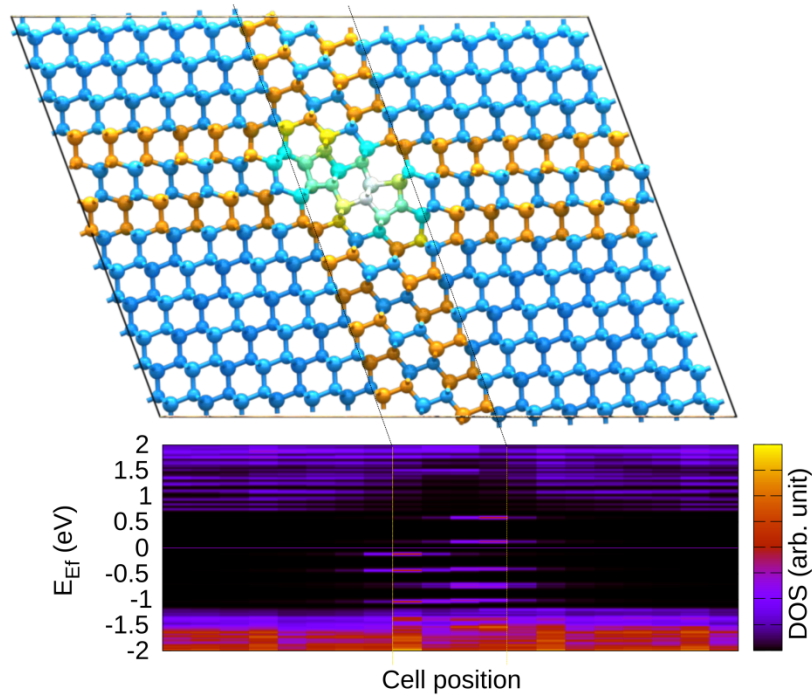


Figure 5: Electronic density of states (integrated in boxes) for the intersection between double SFs, whose atomistic model is illustrated in the top graph. A central slice of the simulated cell, centred at the crossing point, is marked by dotted lines, and also highlight the corresponding position in the DOS plot. The colours of the atomistic structure agree with the previous images.

4. Conclusion

MD simulations were performed to reveal the atomistic behavior at the crossing point of two adjacent partial dislocation loops that are opening along the same $\langle 110 \rangle$ direction in two different $\{111\}$ planes. A pinning-depinning process turns to be activated leading to the formation of a complex junction defect formed by four close 90° dislocation segments parallel to each other. Such configuration has been analysed and associated with the so-called dislocation forest. Moreover, superior ab-initio calculations showed that the resulting structure of the junction does not cause defect states in the electronic bandgap of the material. On the other hand, supposing that the same mechanism is activated also at the intersection of double plane dislocation loops (hence of double plane stacking faults), we constructed another complex defect formed by 30° and 90° parallel and close dislocation segments. The DOS calculated for this junction of double dislocation loops reveals several intra-gap defect states, which are very likely detrimental to the properties of the devices. To our knowledge this work

is the first attempt to model at the atomistic level forest dislocations and predict their impact on the electronic properties of the material.

References

- [1] D. J. Young, J. Du, C. A. Zorman, W. H. Ko, *IEEE Sens. J.* **2004**, *4*, 464.
- [2] S. E. Saddow, A. Agarwal, *Advances in Silicon Carbide Processing and Applications*, Artech House Publisher, Boston **2004**.
- [3] T. J. Fawcett, J. T. Wolan, *Appl. Phys. Lett.* **2006**, *89*, 182102.
- [4] V. V. Afanasev, M. Bassler, G. Pensl, M. Schulz, *Phys. Status Solidi A* **1997**, *162*, 321.
- [5] M. Mehregany, C. A. Zorman, S. Roy, A. J. Fleischman, C. H. Wu, N. Rajan, *Int. Mater. Rev.* **2000**, *45*, 85.
- [6] A. Mantzari, A. Andreadou, M. Marinova, E. K. Polychroniadis, *Acta Phys. Polonica A* **2012**, *121*, 187.
- [7] M. Bhatnagar, B. J. Baliga, *IEEE Trans. Dev.* **1993**, *40*, 645.
- [8] G. Harris, *Properties of Silicon Carbide*, EMIS Datareviews Series, INSPEC, Institution of Electrical Engineers, London **1995**.
- [9] F. Ciobanu, G. Pensl, H. Nagasawa, A. Schöner, S. Dimitrijević, K. Y. Cheong, V. V. Afanas'ev, G. Wagner, *Mater. Sci. Forum* **2003**, *433*, 551.
- [10] S. Nishino, J. A. Powell, H. A. Will, *Appl. Phys. Lett.* **1983**, *42*, 460.
- [11] P. Pirouz, C. M. Chorey, T. T. Cheng, J. A. Powell, *MRS Proc.* **1987**, *91*, 399.
- [12] M. E. Levinshstein, S. L. Rumyantsev, M. S. Shur, *Properties of advanced semiconductor materials: GaN, AlN, InN, BN, SiC, SiGe*, Wiley, Hoboken, NJ **2001**.
- [13] C. W. Liu, J. C. Sturm, *J. Appl. Phys.* **1997**, *82*, 4558.
- [14] Y. Ishida, M. Kushibe, T. Takahashi, H. Okumura, S. Yoshida, *Mater. Sci. Forum.* **2002**, *389*, 459.
- [15] M. A. Capano, A. R. Smith, B. C. Kim, E. P. Kvam, S. Tsoi, A. K. Ramdas, J. A. Cooper, *Mater. Sci. Forum* **2006**, *527*, 431.
- [16] H. Nagasawa, K. Yagi, T. Kawahara, N. Hatta, M. Abe, *Microelectron. Eng.* **2006**, *83*, 185.
- [17] J. Eriksson, M. H. Weng, F. Roccaforte, F. Giannazzo, S. Leone, V. Raineri, *Appl. Phys. Lett.* **2009**, *95*, 081907.
- [18] T. Kawahara, N. Hatta, K. Yagi, H. Uchida, M. Kobayashi, M. Abe, H. Nagasawa, B. Zippelius, G. Pensl, *Mater. Sci. Forum* **2010**, *645*, 339.

- [19] H. Nagasawa, T. Kawahara, K. Yagi, N. Hatta, H. Uchida, M. Kobayashi, S. Reshanov, R. Esteve, A. Schöner, *Mater. Sci. Forum* **2012**, 711, 91.
- [20] H. Nagasawa, M. Abe, K. Yagi, T. Kawahara, N. Hatta, *Phys. Status Solidi Basic Res.* **2008**, 245, 1272.
- [21] A. Severino, C. Bongiorno, N. Piluso, M. Italia, M. Camarda, M. Mauceri, G. Condorelli, M. A. Di Stefano, B. Cafra, A. La Magna, F. La Via, *Thin Solid Films* **2010**, 518, S165.
- [22] T. Kreiliger, M. Mauceri, M. Puglisi, F. Mancarella, F. La Via, D. Crippa, W. Kaplan, A. Schöner, A. Marzegalli, L. Miglio, H. von Känel, *Mater. Sci. Forum* **2016**, 858, 151.
- [23] H. von Känel, L. Miglio, D. Crippa, T. Kreiliger, M. Mauceri, M. Puglisi, F. Mancarella, R. Anzalone, N. Piluso, F. La Via, *Mater. Sci. Forum* **2015**, 821, 193.
- [24] F. La Via, A. Severino, R. Anzalone, C. Bongiorno, G. Litrico, M. Mauceri, M. Schoeler, P. Schuh and P. Wellmann, *Mater. Sci. Semicond. Process.* **2018**, 78, 57.
- [25] M. Zimbone, E. G. Barbagiovanni, C. Bongiorno, C. Calabretta, L. Calcagno, G. Fisicaro, A. L. Magna, F. L. Via, *Cryst. Growth Des.* **2020**, 20, 3104.
- [26] G. Fisicaro, C. Bongiorno, I. Deretzis, F. Giannazzo, F. L. Via, F. Roccaforte, M. Zielinski, M. Zimbone, A. La Magna, *Appl. Phys. Rev.* **2020**, 7, 021402.
- [27] H. Nagasawa, R. Gurunathan, M. Suemitsu, *Mater. Sci. Forum* **2015**, 821, 108.
- [28] G. Litrico, R. Anzalone, A. Alberti, C. Bongiorno, G. Nicotra, M. Zimbone, M. Mauceri, S. Coffa, F. La Via, *Mater. Sci. Forum* **2018**, 924, 124.
- [29] A. A. Lebedev, P. L. Abramov, S. P. Lebedev, G. A. Oganessian, A. S. Tregubova, D. V. Shamshur, *Physica B* **2009**, 404, 4758.
- [30] X. Song, J. F. Michaud, F. Cayrel, M. Zielinski, M. Portail, T. Chassagne, E. Collard, D. Alquier, *Appl. Phys. Lett.* **2010**, 96, 142104.
- [31] C. Wen, Y. M. Wang, W. Wan, F. H. Li, J. W. Liang, J. Zou, *J. Appl. Phys.* **2009**, 106, 073522.
- [32] M. Bosi, C. Ferrari, D. Nilsson, P. J. Ward, *CrystEngComm* **2016**, 18, 7478.
- [33] F. La Via, G. D'Arrigo, A. Severino, N. Piluso, M. Mauceri, C. Locke, S. E. Sadow, *J. Mater. Res.* **2013**, 28, 94.
- [34] U. Lindelfelt, H. Iwata, S. Öberg and P. R. Briddon, *Phys. Rev. B: Condens. Matter Mater. Phys.* **2003**, 67, 155204.
- [35] E. Scalise, L. Barbisan, A. Sarikov, F. Montalenti, L. Miglio, A. Marzegalli, *J. Mater. Chem. C* **2020**, 8, 8380.
- [36] L. Barbisan, A. Sarikov, A. Marzegalli, F. Montalenti, L. Miglio, *Phys. Status Solidi B* **2021**, 258, 2000598.

- [37] A. Sarikov, A. Marzegalli, L. Barbisan, M. Zimbone, C. Bongiorno, M. Mauceri, D. Crippa, F. La Via, L. Miglio, *CrystEngComm* **2021**, *23*, 1566.
- [38] M. Zimbone, A. Sarikov, C. Bongiorno, A. Marzegalli, V. Scuderi, C. Calabretta, L. Miglio, F. La Via, *Acta Materialia* **2021**, *213*, 116915.
- [39] S. Plimpton, *J. Comput. Phys.* **1995**, *117*, 1.
- [40] P. Vashishta, R. K. Kalia, A. Nakano, J. P. Rino, *J. Appl. Phys.* **2007**, *101*, 103515.
- [41] A. Sarikov, A. Marzegalli, L. Barbisan, E. Scalise, F. Montalenti, L. Miglio, *Modelling Simul. Mater. Sci. Eng.* **2019**, *28*, 015002.
- [42] W. Shinoda, M. Shiga, M. Mikami, *Phys. Rev. B* **2004**, *69*, 134103.
- [43] A. Stukowski, *Modelling Simul. Mater. Sci. Eng.* **2009**, *18*, 015012.
- [44] J. Hirth, J. Lothe, *Theory of Dislocations*, Krieger Publishing Company, Malabar **1982**.
- [45] L. Tong, M. Mehregany, L. G. Matus, *Appl. Phys. Lett.* **1992**, *60*, 2992.

Acknowledgements

The authors acknowledge EU for funding the CHALLENGE project (3C-SiC Heteroepitaxially grown on silicon compliance substrates and 3C-SiC substrates for sustainable wide-bandgap power devices) within the EU's H2020 framework program for research and innovation under grant agreement no. 720827 and the ISCRA initiative under the CINECA Italian supercomputing facility for the computational resources. We also thank Prof. H. Nagasawa for the fruitful discussions.

Received: ((will be filled in by the editorial staff))

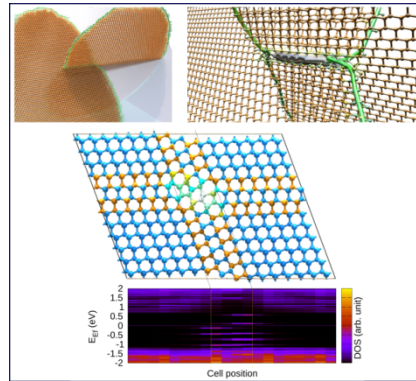
Revised: ((will be filled in by the editorial staff))

Published online: ((will be filled in by the editorial staff))

Table of Contents

Luca Barbisan, Emilio Scalise and Anna Marzegalli*

Evolution and Intersection of Extended Defects and Stacking Faults in 3C-SiC Layers on Si (001) Substrates by Molecular Dynamics Simulations: The Forest Dislocation Case



A synergic approach based on classical molecular dynamic and first-principles simulations is used to investigate the process activated at the intersection of evolving dislocation loops in 3C-SiC. We reveal the atomistic configuration of the defects formed and the consequent detrimental impact on the electronic properties of 3C-SiC, particularly for the intersection of two double dislocations loops.